Novel organometallic chloroquine derivative inhibits tumor growth

Elizabeth A. Hall[1,2] | Jon E. Ramsey[1,3] | Zhihua Peng[1,2] | Davit Hayrapetyan[4] | Viacheslav Shkepu[4] | Bruce O'Rourke[5] | William Geiger[1,5] | Kevin Lam[1,4,6] | Claire F. Verschraegen[1,7]

[1] The University of Vermont Cancer Center, Burlington, Vermont
[2] Department of Medicine, The University of Vermont, Burlington, Vermont
[3] Department of Biochemistry, The University of Vermont, Burlington, Vermont
[4] Department of Chemistry, Nazarbayev University, Astana, Republic of Kazakhstan
[5] Department of Chemistry, The University of Vermont, Burlington, Vermont
[6] Department of Pharmaceutical, Chemical and Environmental Sciences, Faculty of Engineering and Science, University of Greenwich, Chatham Maritime, Chatham, Kent, United Kingdom
[7] Department of Internal Medicine, Division of Medical Oncology, The Ohio State University Comprehensive Cancer Center, Columbus, Ohio

Correspondence
Jon E. Ramsey, Department of Biochemistry, University of Vermont, 89 Beaumont Avenue, Given E213, Burlington 05405, VT.
Email: jeramsey@uvm.edu

Funding information
Irvin Krakoff Professor of Medicine Endowment; SPARK-VT program; Lake Champlain Cancer Research Organization Research Fellowship; Nazarbayev University ORAU; Ministry of Education and Science of Kazakhstan

Abstract

Autophagy has emerged as a mechanism critical to both tumorigenesis and development of resistance to multiple lines of anti-cancer therapy. Therefore, targeting autophagy and alternative cell death pathways has arisen as a viable strategy for refractory tumors. The anti-malarial 4-aminoquinoline compounds chloroquine and hydroxychloroquine are currently being considered for re-purposing as anti-cancer therapies intended to sensitize different tumors by targeting the lysosomal cell death pathway. Here, we describe a novel organometallic chloroquine derivative, cymanquine, that exhibits enhanced bioactivity compared to chloroquine in both normal, and reduced pH tumor microenvironments, thus overcoming a defined limitation of traditional 4-aminoquinolines. In vitro, cymanquine exhibits greater potency than CQ in a diverse panel of human cancer cell lines, including melanoma, in both normal pH and in reduced pH conditions that mimic the tumor microenvironment. Cymanquine treatment results in greater lysosomal accumulation than chloroquine and induces lysosomal dysfunction leading to autophagy blockade. Using a mouse model of vemurafenib-resistant melanoma, cymanquine slowed tumor growth greater than hydroxychloroquine, and when used in combination with vemurafenib, cymanquine partially restored sensitivity to vemurafenib. Overall, we show that cymanquine exhibits superior lysosomal accumulation and autophagy blockade than either chloroquine or hydroxychloroquine in vitro; and in addition to its high level of tolerability in mice, exhibits superior in vivo efficacy in a model of human melanoma.

KEYWORDS

autophagy, chloroquine, lysosome, melanoma, vemurafenib-resistance

1 | INTRODUCTION

Autophagy is a catabolic cellular salvage pathway by which cells degrade and recycle organelles and macromolecular remnants to regenerate molecular constituents for anabolic metabolism and to satisfy energy requirements. Autophagy involves initial sequestration of cellular components into membrane-bound vesicles that fuse with low pH lysosomes,

leading to their degradation. Both healthy and malignant cells utilize autophagy, but in rapidly dividing tumor cells, autophagy increases to meet survival needs in a nutrient-deprived microenvironment.[1–3] Tumor cells rely on autophagy to develop resistance to various targeted agents and chemotherapies. For example, the amount of autophagic flux in melanomas can predict tumor invasiveness, chemotherapeutic resistance, and patient survival.[4] Knockdown of essential autophagy machinery protein genes forces cell death in melanoma cells.[5] Pharmacological inhibition of autophagy re-sensitizes resistant tumor cells to primary targeted therapies.[6,7] Thus, inhibiting autophagy might be an effective way of overcoming drug resistance in various tumor types.[8]

The anti-malarial 4-aminoquinoline compounds, chloroquine (CQ), and its derivative hydroxychloroquine (HCQ), are currently the focus of anticancer repurposing efforts for their ability to inhibit autophagy in various tumor types. CQ and HCQ are amphipathic lysosomotropic agents that diffuse through cellular membranes by virtue of their partial hydrophobic character. Their weak base properties cause them to become protonated in acidic milieu. In their charged, protonated state, CQ, and HCQ become unable to diffuse out of the organelle, causing accumulation within lysosomes.[9] This leads to neutralization of the lysosomal lumen, disruption of lysosomal functions including autophagy, and eventually lysosomal membrane permeabilization, and cell death.[10,11] However, CQ and HCQ have an important limitation. Solid tumors with poor vasculature and insufficient blood flow develop microenvironmental hypoxia, causing them to primarily utilize hypoxic glycolysis for ATP synthesis, resulting in acidic extracellular microenvironments within these solid tumors.[12] Low pH significantly decreases the bioavailable fraction of CQ and HCQ. Additionally, acidic conditions can induce autophagy in cells as a means of survival. This limitation has fueled efforts to develop chloroquine derivatives that can improve the inhibition of autophagy in acidic tumor microenvironments.[13,14]

Bioorganometallic chemistry appeared as a new field in 1985.[15] During its infancy, the field was clearly overshadowed by the supremacy of research on organometallic catalysts since it was assumed that organometallic complexes were incompatible with oxygen and water and, thus, unsuitable for use in biological systems. However, the bioorganometallic field has flourished with the design of remarkably bioactive organometallics such as ferroquine (iron-based antimalarial, derived from CQ),[16] ferrocifen (iron-based anti-breast cancer, derived from tamoxifen),[17] and Ru-metronidazole (ruthenium-based bacterial topoisomerase II inhibitor, derived from metronidazole).[18]

We characterize the anticancer activity of a newly described organometallic CQ derivative called Cymanquine (CMQ).[19,20] CMQ is a CQ derivative containing a cymantrene substitution that leads to greater cytotoxic activity in vitro to tumor cells compared to traditional quinolines, in both low and normal pH environments. The apparent mechanism for cytotoxicity is supported by data showing increased lysosomal accumulation and disruption of lysosome-dependent autophagy. Consistent with in vitro studies showing greater cytotoxicity, CMQ displays effectiveness as a single agent in slowing tumor growth in a mouse model of human melanoma.

2 | MATERIALS AND METHODS

2.1 | Synthesis of compounds

Cymanquine (compound 4, Figure 1), pseudocymanquine (compound 5, Figure 1) and ferroquine (compound 3,

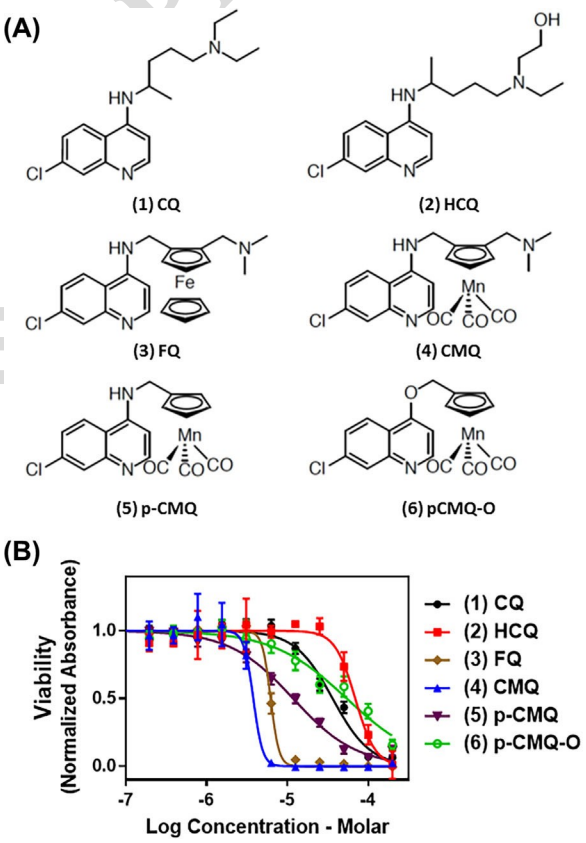

FIGURE 1 CMQ exhibits greater potency than traditional 4-aminoquinolines and other organometallic CQ derivatives. A, structures of parent compound CQ: (1) and its derivatives: HCQ; (2), ferroquine (3); CMQ; (4), pseudo-CMQ; (5), pseudo-CMQ-O; and (6). B, cell viability (MTS) assay to determine cytotoxic activity of test compounds

Figure 1) were synthesized as previously described.[19,21] A complete description of the synthesis of O-pseudocymanquine (pCMQ-O, compound 6, Figure 1) can be found in Supplementary Information.

2.2 | Cell lines and reagents

Human cancer cell lines ACHN (CRL-1611), BxPC3 (CRL-1687), DU145 (HTB-81), HT29 (HTB-38), Jurkat (TIB-152), LNCaP (CRL-1740), PC3 (CRL-1435), SB1A, A375 (CRL-3224), and T47D (HTB-133) were cultured in RPMI 1640 ([Q4]Corning-Cellgro #10-1040-CV) supplemented with 10% FBS (SH30910.3), 1% penicillin/streptomycin/amphotericin B solution (SV30079.01), 1 mM sodium pyruvate (SH30239.01), 1% MEM non-essential amino acid solution (SH30238.1), and 2 mM L-glutamine (SH30034.01) at 37°C in a 5% CO_2, humidified incubator. All supplements were purchased from HyClone™ (Logan, UT). The HPV-18-transformed normal human prostate epithelium cell line, RWPE-1 (a gift of Dr. Jane B. Lian, University of Vermont) was cultured in Keratinocyte-SFM (Thermo Fisher Scientific #17005-042) supplemented with 5 ng/mL human recombinant epidermal growth factor (Thermo Fisher Scientific #PHG0311), and 50 μg/mL bovine pituitary extract (Life Technologies #13028014) at 37°C in a 5% CO_2, humidified incubator. All cancer cell lines were acquired from the American Type Culture Collection with the exception of SB1A, which has been described previously.[22] All cell line cultures were tested as negative for Mycoplasma contamination using the MycoAlert Mycoplasma Detection Kit (Lonza #LT07-118), and were used for experimentation within five passages of thawing. Chloroquine diphosphate (MP Biomedicals, LLC #193919) and hydroxychloroquine (Selleck Chemicals #S4430) stock solutions were prepared in water, and organometallic compounds were all prepared in dimethylsulfoxide (DMSO, EMD Millipore #MX1458-6), all at a concentration of 10 mM. Vemurafenib-resistant A375 melanoma cells were generated by plating A375 cells in a 10 cm dish in the presence of increasing concentrations of Vemurafenib (LC Laboratories #V-2800) in DMSO, starting with 1 μM. Resistant clones were maintained in 2 μM Vemurafenib.

2.3 | Cytotoxicity assay

Cells were plated in quadruplicate in 96-well tissue culture plates (Falcon) at a density of 2000-5000 cells per well (depending upon growth rate of cell line) in a volume of 100 μL growth media. Cells were then incubated in the presence of test compounds for 72 h. Viability was measured by the CellTiter 96 aqueous non-radioactive cell proliferation assay (Promega, Madison, WI, #G5430) per manufacturer's instruction. Absorbance was measured on a Perkin-Elmer Victor ×4 multi-label plate reader. Absorbance data was fit to a four parameter inhibitor response model using Prism software (GraphPad Software, La Jolla, CA) to obtain IC_{50} values and normalization parameters. Statistical analyses were also performed using Prism software.

2.4 | Western blotting

See Supplementary Information for a complete description of Western blotting methods and materials.

2.5 | Flow cytometry

For concurrent lysosomal staining and cytotoxicity measurement, a flow cytometric adaptation of previously published methods[23] was employed. For measurement of autophagic flux, a fluorescent reporter (DsRed-LC3-GFP)-based flow cytometry method was used as described.[24,25] The retroviral plasmid used for expression of the reporter, pQCXI-Puro-DsRed-LC3-GFP, was a gift from David Sabatini (Addgene plasmid # 31182). A more detailed description of the method employed here can be found in Supplementary Information.

2.6 | Fluorescence microscopy

To achieve expression of fluorescent-labeled LC3 to enable fluorescence microscopy detection of subcellular localization, an exogenous EGFP-LC3 fusion construct was obtained as a gift from Karla Kirkegaard (Addgene plasmid #11546).[26] The plasmid was transfected into cell line PC3 with Lipofectamine 3000 reagent (Thermo Fisher Scientific #L3000008), expanded under neomycin selection, and plated on Nunc Lab-Tek II chamber slides. Cells were treated with drugs for 6 h prior to washing and fixation using 2% paraformaldehyde in PBS. Cells were visualized on a Zeiss Axio Imager 2 fluorescence microscope equipped with a Hamamatsu CCD camera.

2.7 | Lysosome isolation

Briefly, lysosome isolation was carried out by differential centrifugation. See Supplementary Information for a complete description of Lysosome Isolation.

2.8 | Liquid chromatography/mass spectrometry

Quantitation of test compounds from biological materials was performed by high performance liquid chromatography/mass spectrometry (HPLC-MS/MS). For a detailed description of methods used for HPLC-MS/MS, see Supplementary Information.

2.9 | Animal models

All animal work was performed under approval and supervision of the University of Vermont Institutional Animal Care and Use Committee (IACUC). A complete description of methods involving animal models can be found in Supplementary Information.

3 | RESULTS

3.1 | CMQ exhibits more potent cytotoxicity compared to CQ and other quinoline derivatives

To examine if novel organometallic substitutions on the quinoline framework could confer increased efficacy in low pH environments, we tested a panel of traditional quinolines, CQ (compound 1) and HCQ (compound 2), and several novel organometallic CQ derivatives, whose structures are shown in Figure 1A. Our previous experience in replacing a ferrocene group by a cymantrenyl center ($CpMn(CO)_3$)[27] prompted us to prepare cymanquine based on the previously described ferroquine (FQ, compound 3).

Therefore, we tested the potent antimalarial organometallic quinoline, FQ, which is an effective agent for targeting CQ-resistant malarial parasites,[21] but for which mammalian anti-cancer activity has not been described. We tested CMQ (compound 4). We then also prepared analogues with decreased basicity such as a CMQ derivative in which one of the basic group, the trimethylamine group has been removed (termed pseudocymanquine, or p-CMQ; compound 5), and a 4-oxoquinoline derivative of p-CMQ termed pCMQ-O (compound 6) where two basic sites have been removed (the triethylamine and the aniline groups.We measured the cytotoxic activity of these compounds in the melanoma cell line A375 (Figure 1B). Results from this strategy showed that both FQ and CMQ displayed a lower IC_{50} than CQ or HCQ by at least an order of magnitude, with CMQ showing the highest potency of all compounds tested.

3.2 | CMQ exhibits greater potency than CQ in both normal and low pH environments

We systematically treated cell lines grown in both normal and low pH conditions with a range of CMQ or CQ concentrations. After 72 h of exposure to drug, cell viability was assessed by the MTS assay. Viability curves like those shown in Figure 2A were fit to an inhibition model to determine the IC_{50}. As summarized in Figure 2B, and detailed in Table 1, CMQ exhibited more greater potency than CQ across all cell lines tested, as indicated by lower pairwise IC_{50} values in both normal and low pH settings. The IC_{50} offset created by low pH conditions was not observed for CMQ to the extent

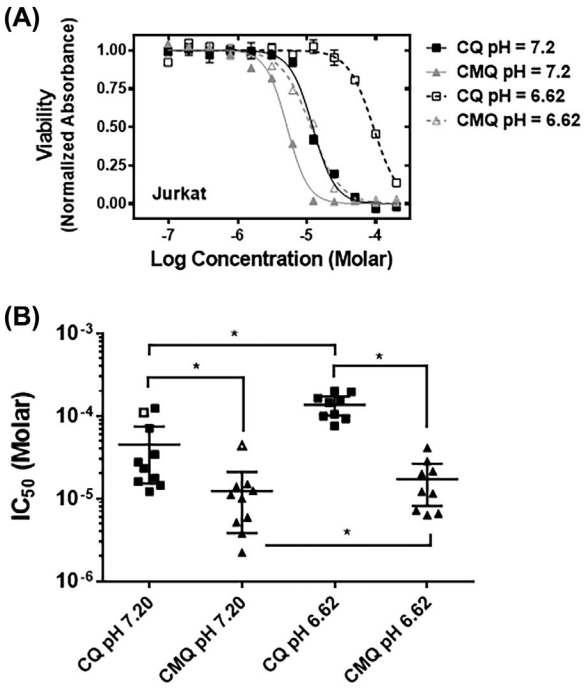

FIGURE 2 CMQ has greater potency than CQ in both normal and low pH environments in diverse human cancer cell lines. A, representative dose-response cell viability assay (MTS assay) for human lymphoma cell line, Jurkat, exposed to CMQ, and CQ for 72 h, in normal and low pH settings (mean ± SEM [n = 4]). B, aggregate IC_{50} values in a diverse panel of cell lines in both normal and low pH settings after 72 h of exposure to CMQ and CQ. Symbols represent best-fit IC_{50} values. Lines represent mean and 95% confidence intervals. Paired t-tests were performed to evaluate statistical significance (*$P < 0.05$). #, Culturing of this cell line was not amenable to low pH conditions

that it was for CQ. The normal prostate epithelial cell line, RWPE-1, was included to show relative sensitivity compared to transformed cell lines. RWPE-1 was most resistant to both CQ and CMQ exposure, suggesting that transformed cells are more dependent upon autophagy than their non-transformed counterparts. However, we cannot rule out differences in sensitivity being owed to differences in the formulations in the growth media employed. CQ displayed an average IC_{50} of 26.1 μM for all cell lines tested at normal pH, and an average of 141 μM at low pH. CMQ displayed an average IC_{50} of 7.53 μM at normal pH, and an average of 14.2 μM at low pH. These findings suggest that CMQ may act as a more potent lysosomal inhibitor in bulky solid tumors, where tumor interior acidification has been observed to augment autophagic flux, particularly in melanoma.[12] We hypothesize that the comparatively higher activities observed for CMQ versus CQ are due to the aforementioned pK_a differences and correspondingly higher bioavailable fractions of the drug (uncharged CMQ) at both pH values tested. This is of

TABLE 1 Potency (IC_{50} (95% confidence limits) of CQ versus CMQ in cell lines grown in normal and low pH conditions

Cell line	CQ pH 7.20	CMQ pH 7.20	CQ pH 6.62	CMQ pH 6.62
ACHN	34.1 (18.0-64.4)	10.1 (8.16-12.6)	201 (Very wide)[a]	41.3 (34.8-49.1)
BxPC3	17.7 (15.8-19.9)	5.94 (5.55-6.35)	75.5 (55.1-103)	7.18 (6.49-7.96)
DU145	71.5 (63.1-80.9)	11.1 (10.1-12.9)	197 (156-248)	28.5 (21.2-38.4)
HT29	14.5 (9.56-21.9)	3.78 (2.88- 4.97)	99.6 (65.4-152)	6.64 (5.10-8.64)
Jurkat	12.2 (10.5-14.2)	5.18 (4.52-5.95)	92.3 (66.8-128)	11.5 (9.51-13.8)
LNCaP	75.0 (62.2-90.4)	14.9 (13.2-16.8)	165 (110-248)	12.2 (9.99-14.8)
SB1A	16.1 (9.77-26.6)	2.23 (1.88-2.64)	105 (Very wide)	6.34 (6.12-6.62)
PC3	23.2 (11.6-47.4)	12.5 (10.4-15.1)	154 (118-201)	21.5 (16.4-28.1)
T47D	27.6 (15.3-49.9)	14.0 (9.37-20.9)	145 (137-154)	20.0 (16.6-24.2)
RWPE1	110 (106-114)	43.9 (40.4-47.8)	N/A[b]	N/A[b]

[a]Ambiguous fit to inhibition model did not permit finite determination of 95% confidence intervals.
[b]The RWPE1 cell line was not compatible with low pH growth conditions.

particular importance since low pH conditions have been identified as a major in vivo limitation for CQ and HCQ.[12]

3.3 | CMQ has greater lysosomotropic activity than CQ

Since our in vitro cytotoxicity studies demonstrated that CMQ outperforms traditional quinolones at killing cancer cells, we sought to determine whether CMQ shared a similar mechanism of action with CQ and HCQ. CQ and HCQ accumulate in lysosomal compartments and disrupt lysosomal functions, including lysosome-associated autophagy, although these compounds may also be inhibiting other cellular processes that are dependent upon lysosomal integrity.[28,29] To determine whether differences between CMQ and CQ cytotoxic activity were due to biovailability and subsequent accumulation of these compounds in various cellular compartments, we used a cell fractionation approach coupled with high sensitivity measurement of drug analytes by HPLC-MS/MS. Figure 3A demonstrates the extent of lysosomal enrichment achieved from SB1A melanoma cells treated for 16 h with 1 μM CMQ or CQ, using differential ultracentrifugation. The lysosomal marker LAMP2 was used as an indicator of enrichment from fractions with equal total protein content. These fractions of equal total protein content were then analyzed by HPLC-MS/MS to determine drug concentrations in each fraction. CMQ had over 50-fold greater accumulation in lysosomes than CQ and over six-fold greater accumulation in whole cell and nuclear fractions (Figure 3B).

We co-stained treated cells with the lysosomotropic fluorophore NBD-PZ and propidium iodide to simultaneously measure lysosomal content and cell viability by flow cytometry, and applying a gating algorithm as shown in Figure 3C. Live cells were sorted based on the absence of propidium iodide staining (Figure 3C, left panel). Live cells, analyzed for staining with the lysosomotropic fluorophore NBD-PZ, showed higher fluorescence intensity in cells treated with CMQ and correspondingly, higher lysosomal accumulation (Figure 3C, right panel). Treatment with low micromolar concentrations of CMQ caused significant cytotoxicity within 24 h, not merely cytostatic activity as evidenced by the presence of dead (PI positive) cells, whereas treatment with CQ did not (Figure 3D). CMQ-induced cytotoxicity is accompanied by significantly higher lysosomal accumulation compared to CQ treated cells (Figure 3E), as measured by NBD-PZ median fluorescence intensity. As stated, at the highest concentration of CMQ tested, NBD-PZ fluorescence intensity becomes reduced, and not significantly different from CQ, because of increasing cell death with CMQ. This approach cannot discriminate between decrease in lysosomal content and an increase in lysosomal pH, since emission of NBD-PZ depends on both fluorophore concentration and pH. The possibility exists that lysosomal content is increased by high CMQ concentrations but the lysosomal lumens are simultaneously becoming neutralized. Despite this caveat, the results show that CMQ accumulates in cells to a greater extent than CQ when cells are exposed to equimolar concentrations of either drug, and that the lysosomes appear to be the primary site of accumulation of both drugs. Additionally, CMQ exposure causes an accumulation of lysosomes in living cells and has more potent cytotoxic activity than CQ over a 24 h period.

3.4 | CMQ disrupts lysosome-dependent autophagy

Lysosomal function is required for autophagy to proceed. We used the conventional method of following the accumulation

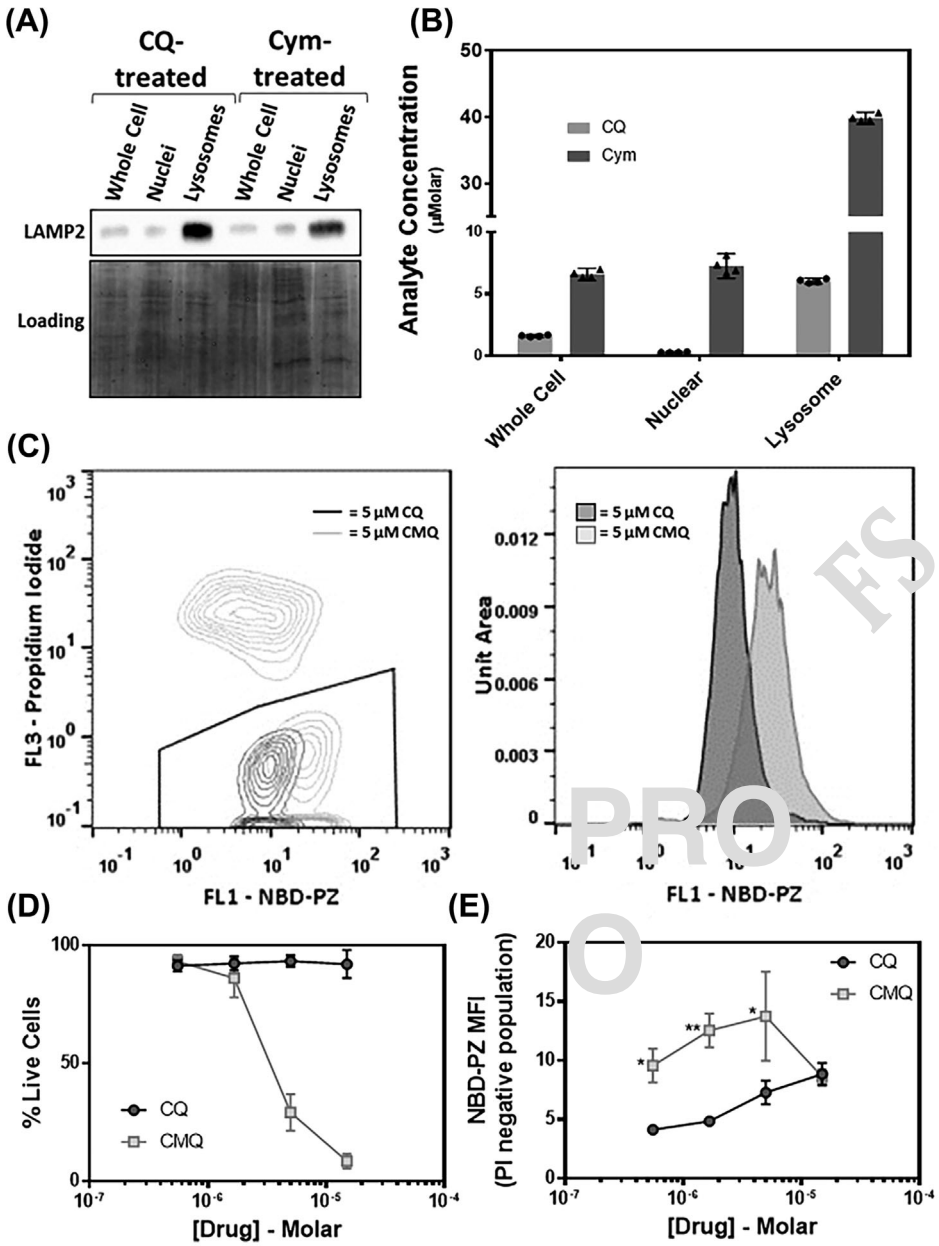

FIGURE 3 CMQ displays greater lysosomal accumulation than CQ. SB1A melanoma cells treated with 1 μM CQ or CMQ for 24 h, underwent cellular fractionation by differentiation centrifugation. A, fractionation was confirmed by Western blot. B, drug concentration in each fraction was quantified via HPLC-MS/MS analysis. C, after 24 h of exposure to 5 μM CMQ or CQ, SB1A cells were simultaneously stained with NBD-PZ and propidium iodide and analyzed by flow cytometry. Live cells were sorted based on absence of propidium iodide staining (left panel, pentagonal gate), then analyzed for NBD-PZ staining (right panel), which is indicative of lysosomal content. D, dose-response cell viability curves after exposure to various concentrations of CQ and CMQ measured as percentage of live cells (negative for propidium iodide staining). E, NBD-PZ median fluorescence intensity reflecting lysosomal content and acidity, as NBD-PZ emission depends on pH. Data in (D and E) presented as mean ± SEM ($n = 3$). $^{*}P < 0.05$ and $^{**}P < 0.001$ by student's t-test

of ubiquitin-like autophagy-related proteins and autophagy cargo adapter proteins to survey autophagic flux in cells treated with either CQ or CMQ. Lipidation of the ubiquitin-like proteins microtubule associated protein-light chain 3 (MAP-LC3, or referred to here as LC3) and γ-aminobutyric acid-type-A-receptor-associated protein (GABARAP) are important steps in autophagosome elongation.[30] It is well established that elongation steps becomes stalled in the presence of lysosomotropic agents, like CQ and HCQ.[31,32] Additionally, trafficking of specified substrates to the autophagosome is carried out by cargo adaptor proteins, such as p62/SQSTM1 (hereafter referred to as p62), that

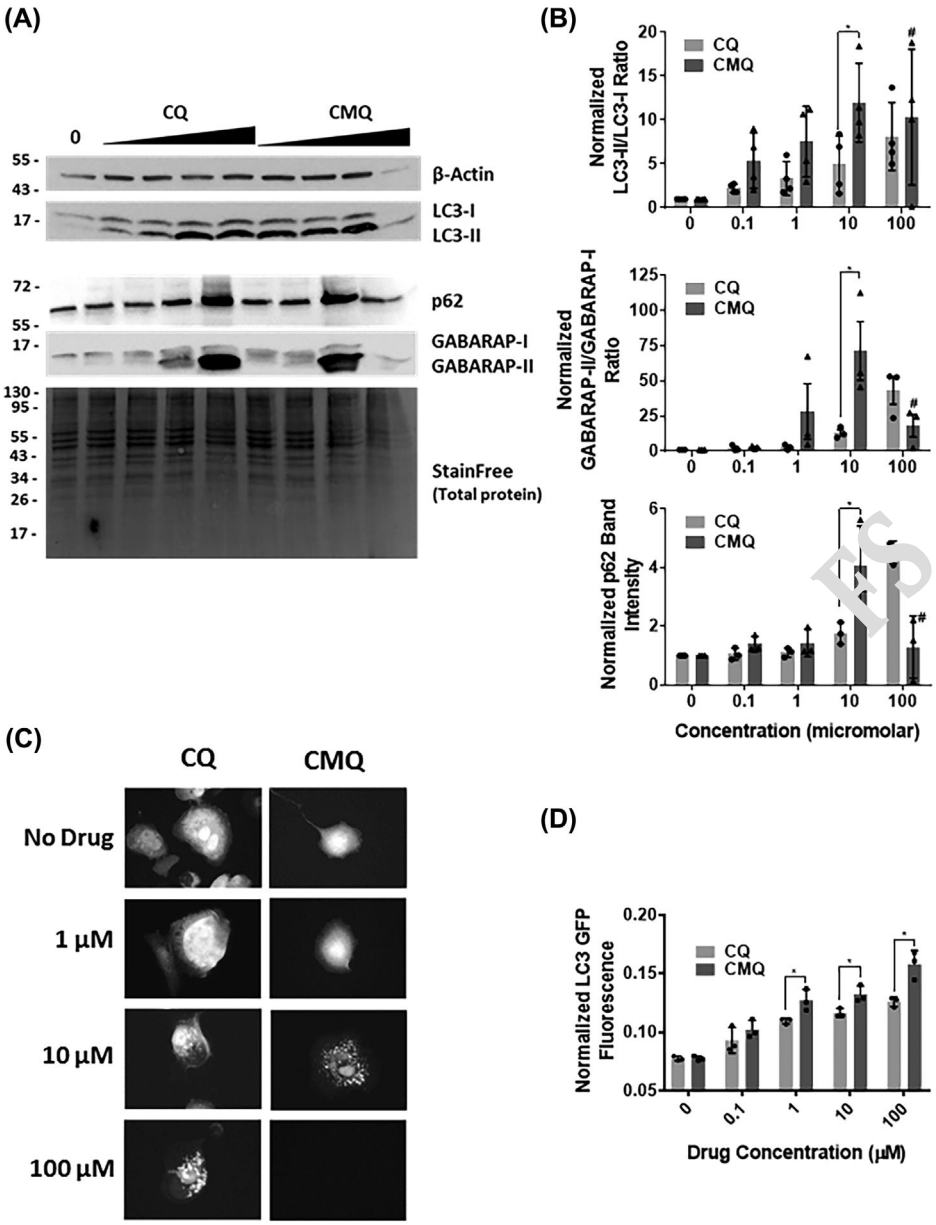

FIGURE 4 Mechanisms of CMQ-induced cytotoxicity includes autophagy blockade. A, SB1A cells were treated with various concentrations of CQ or CMQ for 24 h prior to Western blotting for LC3 and GABARAP isoforms I and II, and for p62. B, densitometry of protein bands was performed to determine LC3-II/I and GABARAP-II/I ratios and p62 accumulation. Bars represent mean values ± SEM from three replicate experiments (*$P < 0.05$). #, indicates cell death. C, PC-3 cells stably expressing EGFP-LC3 were treated with CQ or CMQ for 4 h prior to fluorescence microscopy evaluation of EGFP-LC3 subcellular deposition. Punctate LC3 distribution is indicative of autophagy blockade. D, authopagic flux was evaluated by flow cytometry-based measurement of DsRed-LC3-GFP reporter fluorescence as a consequence of CQ or CMQ treatment. Cells were treated with indicated concentrations of drugs 24 h prior to analysis. Bars represent mean values ± SEM from three replicate experiments (*$P < 0.05$)

accumulate upon autophagy disruption. We monitored this process by Western blot to observe the effects of CMQ on accumulation of lapidated isoforms of LC3 and GABRAP (LC3-II, and GABARAP-II, respectively), and overall p62 levels using CQ as a positive/comparative control. SB1A cells were treated with various concentrations of CMQ or CQ for 24 h prior to western analysis. CMQ treatment results in higher levels of LC3-II, p62, and GABARAP-II accumulation at lower concentrations compared to CQ as shown in Figure 4A. Quantitative analysis of Western blot data was performed (Figure 4B) shows that significantly higher ratios of LC3-II/LC3-I and GABARAP-II/GABARAP-I, and p62 levels are obtained in cells treated with CMQ compared to CQ, at 10 µM final concentrations. Excessive cell death was

observed in cells treated with 100 μM CMQ (marked with # symbol) which led to highly inconsistent results.

To further assess autophagy disruption, PC-3 prostate cancer cells, which stably express the fluorescent EGFP-LC3 fusion protein, were treated with concentrations of either CQ or CMQ for 4 h prior to visualization by fluorescence microscopy. CMQ altered the subcellular distribution of EGFP-LC3 fusion protein resulting in punctate EGFP-LC3 emission pattern, which is a hallmark of autophagy blockade attributable to lysosomal dysfunction[33] (Figure 4C). CMQ and CQ both exhibited punctate LC3 distribution, but the appearance of LC3 puncta are visible at lower CMQ concentrations, consistent with more potent autophagy blockade.

As a last measure of autophagy disruption, we monitored changes in autophagic flux resulting from CQ or CMQ treatment using a flow cytometry-based fluorescent LC3 reporter assay.[24] In this assay, a dual labelled LC3 reporter (DsRed-LC3-GFP) is stably expressed to allow concomitant measurement of autophagic proteolytic activity and internal normalization to overall LC3 expression. In untreated cells the GFP tag is selectively proteolyzed through autophagy. As shown in Figure 4D, treatment of SB1A cells stably expressing the DsRed-LC3-GFP reporter showed increasing levels of normalized GFP fluorescence when treated with CQ or CMQ, indicative of reporter accumulation as a result of autophagy inhibition. CMQ showed significantly higher levels of GFP accumulation than CQ at concentrations greater than 0.1 μM.

These results demonstrate that CMQ disrupts lysosome-dependent autophagy, which may induce cell death through lysosome-mediated cell death pathways.

35 | CMQ displays single agent anti-tumor activity in a mouse model of human melanoma

The promising anti-cancer properties displayed by CMQ in vitro led us to ask whether the compound would be both tolerated and have activity in vivo, in mouse xenograft models. Tolerability was assessed using a dose escalation method with animals receiving doses injected IP on a 3-day-on/2-day-off schedule for a total of 12 days. At all dose levels tested, we observed no behavioral, gross physiological changes, or deaths that would prompt removal of the animals from the experiment. No statistically significant body mass changes were observed (Figure 5A). A trend of body mass loss was observed for the 100 nmole/g cohort, however, this loss was not found to be statistically significant, nor was it

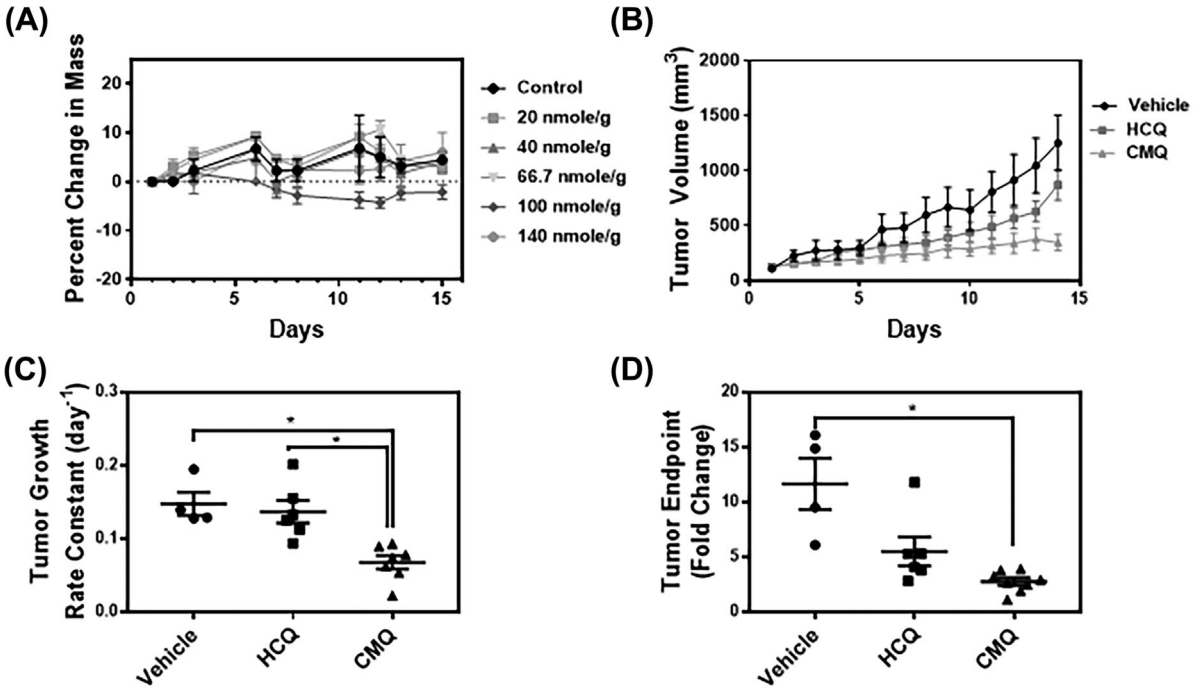

FIGURE 5 CMQ is superior to HCQ as single agent therapy for melanoma in mouse model. A, MTD determination was attempted in female Nu/Nu by a dose escalation strategy whereby body mass was monitored to detect adverse body mass loss. B, A375 xenografts were created in Nu/Nu mice. Efficacy of single agent therapy with CMQ, HCQ, or vehicle on tumor growth. Symbols represent mean tumor volumes ± SEM. C, rates of tumor growth for each drug as a single agent indicate superior efficacy by CMQ on tumor growth. D, relative tumor volumes at endpoint (14 days of treatment) were calculated. In (C and D) lines represent mean ± SEM. Unpaired *t*-tests were performed to determine statistical significance (*$P < 0.05$)

observed at the higher dosing level of 140 nmole/g. The dose escalation experiment did not capture the MTD for CMQ, as we did not exceed 140 nmole/g due to solubility issues. Therefore, all subsequent in vivo experimentation involving CMQ and HCQ was performed at this dosing level.

To assess efficacy of CMQ as an anti-cancer therapeutic, we generated vemurafenib-resistant A375 ($A375^{VR}$) xenograft tumors in female Nu/Nu mice and randomly assigned these mice into three treatment arms: vehicle ($n = 4$), HCQ ($n = 5$), and CMQ ($n = 6$). Both HCQ and CMQ significantly slowed tumor growth compared to vehicle, with CMQ exhibiting slight improvement over HCQ (Figure 5B). Tumor growth inhibition was evaluated by a growth rate analysis approach [34]. HCQ significantly decreased the rate of tumor growth compared to vehicle, but CMQ showed a greater magnitude of tumor growth inhibition compared to both vehicle and HCQ (Figure 5C). The mean tumor volume by day 14 of treatment (endpoint) was 1251 mm^3 for the vehicle group, 869.9 mm^3 for HCQ group, and 275.3 mm^3 for the CMQ group. Analysis of relative tumor volumes at endpoint (Figure 5D) showed that both HCQ and CMQ reduced final tumor volumes at endpoint.

3.6 | CMQ restores sensitivity in vemurafenib-resistant melanoma

Since CMQ exhibited greater potency than CQ and HCQ as a single agent, we also evaluated whether CMQ could reverse drug resistance. $BRAF^{V600E}$-positive human melanoma cell line A375 ^{P}($A375^{P}$ denotes parental line) was exposed to progressively increasing concentrations of vemurafenib over a course several months to create a vemurafenib-resistant cell line ($A375^{VR}$). Resistance was confirmed by evaluating vemurafenib sensitivity in a viability/cytotoxicity assay, where we observed an increase in vemurafenib IC_{50} from approximately 300 nM to greater than 30 μM (Figure 6A). To determine if drug resistance could be reversed by CMQ, as has been reported for HCQ,[7] vemurafenib sensitivity of $A375^{VR}$ was re-determined in the presence of various concentrations of HCQ or CMQ. Both CMQ and HCQ were able to partially restore sensitivity to vemurafenib (Figure 6A); however, CMQ showed a greater ability to reverse vemurafenib resistance at lower concentrations than HCQ (Figure 6).

To evaluate if CMQ can restore vemurafenib sensitivity in vivo, we tested combination therapies in a xenograft model of vemurafenib resistance. All mice received vemurafenib once tumor volumes reached 100 mm^3 plus either vehicle ($n = 4$), HCQ ($n = 4$), or CMQ ($n = 5$). The rate of tumor growth of mice treated with vehicle plus vemurafenib was higher than those treated with vemurafenib plus either HCQ or CMQ (Figure 6C). While the combination of HCQ or CMQ with vemurafenib both slowed tumor growth compared to vemurafenib alone, the rate of tumor growth was slowed to a greater extent in mice treated with vemurafenib plus CMQ (Figure 6D). The mean relative tumor size by day 14 of treatment (endpoint) was 850 mm^3 for the vemurafenib-alone group, compared to 326 mm^3 and 281 mm^3 for vemurafenib plus HCQ and Vemurafenib plus CMQ, respectively. Analysis of relative tumor volumes at endpoint (Figure 6E) showed that while both HCQ and CMQ appeared to reduce final tumor volumes at endpoint, neither achieved the statistical significance threshold implemented ($P < 0.05$). CMQ nearly reached this threshold value with $P = 0.052$.

4 | DISCUSSION

Autophagy plays decisive roles in tumor progression, tumor adaptation, and drug resistance. The use of weak-base lysosomotropics is being tested in clinical trials to slow tumor growth, boost therapeutic efficacy, and reverse drug resistance.[35–39] The weak base character of many lysosomotropic inhibitors represents a worrisome limitation for these drugs, as they are much less potent in acidic milieu.[12] CMQ shares structural and chemical similarities to the novel antimalarial compound, ferroquine (FQ) which has displayed promising results in treating drug-resistant malaria.[40,41] The application of FQ as anticancer therapy has not been reported at the time of this report. The ferrocene substitution in FQ causes a reduction in the pKa and an increase in the lipophilicity of the drug compared to CQ at normal pH.[42] We hypothesized that a cymantrene substitution would manifest as higher potency at both normal and reduced pH conditions.

To test our hypothesis, we examined a panel of both traditional, and novel organometallic quinoline compounds to gauge efficacy as anticancer therapeutics. Our results show that, generally, organometallic quinolines possess greater anti-growth properties than the traditional quinolines, with CMQ displaying superior potency in vitro compared to all compounds tested. The relative cytotoxic activity of p-CMQ was rather unexpected, because of the importance of intramolecular hydrogen bonding between the 4-amino and terminal trimethylamine having been reported in FQ, aiding the diffusion through the hydrophobic membranes.[16] Alleviation of the un-partnered H-bond donor, the 4-amino group, in this context, through substitution with an oxygen atom at this position, might be expected to restore activity. However, we observed the opposite effect. Both compounds lacking the terminal trimethylamine group displayed what we interpreted as cytostatic activity, as opposed to cytotoxic activity. This interpretation stems from the steepness of the viability curves, with CMQ, FQ, HCQ, and to a lesser extent, CQ having steep curves, and p-CMQ and p-CMQ-O having sweeping shallow

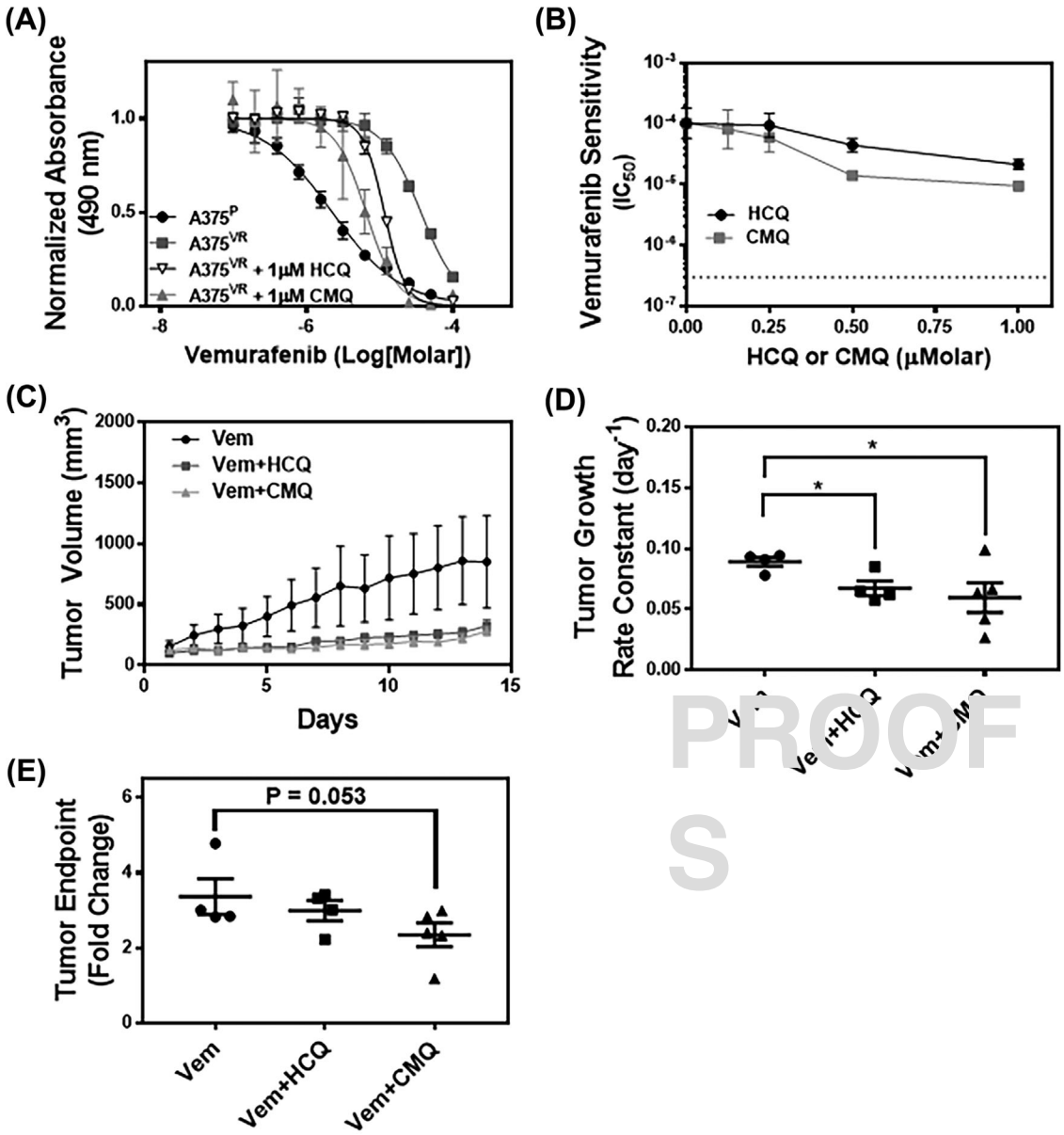

FIGURE 6 CMQ partially restores sensitivity to Vemurafenib in resistant melanoma cells in vivo. A, MTS cytotoxicity assay confirms vemurafenib resistance in A375, as reflected by increased IC_{50} in $A375^{VR}$ compared to A375 parental line ($A375^{P}$). This assay illustrates how addition of HCQ or CMQ affects vemurafenib sensitivity in $A375^{VR}$ cells. B, HCQ and CMQ both partially restore sensitivity to vemurafenib at various concentrations. C, Nu/Nu mouse $A375^{VR}$ xenograft model was used to compare efficacy of HCQ versus CMQ in combination with Vemurafenib on tumor growth. Symbols represent mean tumor volumes ± SEM. D, rates of tumor growth for combination therapy of vemurafenib plus either HCQ or CMQ. Symbols represent best-fit rate constant values of individual tumors. E, relative tumor volumes at endpoint (14 days of treatment) were calculated. In (D and E) lines represent mean ± SEM. Unpaired *t*-tests were performed to determine statistical significance (*$P < 0.05$)

curves indicating progressive growth inhibition over the concentration range spanning the curve (Figure 1).

We compared CMQ's efficacy to that of CQ in a diverse panel of cancer cell lines selected for their ability to adapt and grow in RPMI-1640 supplemented with 10% FBS (Figure 2). Identical growth conditions were essential for our analysis since we postulated that CMQ may inhibit autophagy in a manner similar to CQ and HCQ, and since it has been well-established that cellular metabolism, particularly autophagy, is sensitive to nutrient availabilities and concentrations. Furthermore, RPMI-1640 is a favorable growth medium as it contains lower glucose content than other common growth base media, thus favoring autophagy. Lastly, we were able to modify this medium with PIPES to reproducibly buffer the pH at 6.62 to create growth conditions that mimic the interior of bulky solid tumors.

Using this approach, we observed a consistently lower pairwise IC_{50} value for CMQ compared to CQ in each cell line tested, and that low pH conditions, which diminish CQ activity, have a lesser effect on CMQ. These findings suggest that CMQ may act as a more potent lysosomal inhibitor in bulky solid tumors, where tumor interior acidification has been observed to augment autophagic flux, particularly in melanoma.[12] We hypothesize that the comparatively higher activities observed for CMQ versus CQ are due to the aforementioned pK_a differences and correspondingly higher bioavailable fractions of the drug (uncharged CMQ) at both pH values tested. This is particularly important since low pH conditions are a major in vivo limitation for CQ and HCQ.[12] We observed that those cells most sensitive to CQ exposure were similarly most sensitive to CMQ, whereas those most resistant to CQ were also most resistant to CMQ, implying that both drugs utilize a similar mechanism of action.

A partial understanding of the mechanism of action of antimalarial quinoline compounds in mammalian cells has been in place for decades,[10,43] where it was appreciated that these compounds possessed the capacity to disrupt lysosomal function. This led to their repurposing in the anti-inflammatory armamentarium, where the mechanism of action was elaborated to include disruption of antigen processing through endosome acidification,[44] as well as inhibit Toll-like receptor signaling.[45] Only more recently has the consideration of re-purposing of lysosomotropic compounds entered the anti-cancer field. Disruption of lysosome-dependent autophagy might be therapeutically important, because autophagy is activated in disease progression and severity. The traditional quinolines impact tumor growth primarily through autophagy blockade. Our results show that CMQ maintains the lysosomotropic and anti-autophagy activities of its predecessor molecules, but surpasses them in its ability to accumulate in lysosomes and to prevent autophagy flux (Figure 3).

For CMQ to be considered a viable alternative to CQ or HCQ as an anti-cancer therapy, it must be tolerated, and slow tumor growth in vivo. Our in vivo results demonstrate that CMQ is effective as a single agent in slowing growth of vemurafenib-resistant, $BRAF^{V600E}$-positive human melanoma tumors (Figure 5). Although in vitro results showed that CMQ was superior to HCQ in reversing vemurafenib resistance, the combination of CMQ plus vemurafenib only modestly outperformed the combination of HCQ plus vemurafenib in vivo, as both combinations worked similarly at slowing tumor growth (Figure 6). Furthermore, despite efforts to maintain vemurafenib resistance in our xenograft model, we observed a partial re-establishment of vemurafenib sensitivity, which may have masked differences in the combinatorial efficacy of the added quinolones. We anticipate that inclusion of a HQ-resistant tumor model, such as the 1205 Lu xenograft model shown by McAfee and colleagues to be refractory to HCQ as a single agent[13] might also exasperate efficacy differences between CMQ and HCQ in combination therapy experiments. Additionally, more suitably powered experiments and/or a larger panel of cancer cell lines might reveal more profound differences in CMQ anti-tumor activity compared to HCQ.

Recent studies have highlighted a connection between cancers with mutations in canonical Ras/Raf/Mek/Erk signaling pathways and increased tumorigenesis that is fueled by autophagy.[46–50] These findings prompt further evaluation of lysosomotropic inhibitors of autophagy in cancers possessing these mutations, which account for approximately 30% of all tumors. Further investigation into the effects of CMQ treatment in such tumor types is warranted.

ACKNOWLEDGMENTS

The authors would like to thank the staff of the University of Vermont Mass Spectrometry Facility and the University of Vermont Larner College of Medicine Flow Cytometry & Sorting Facility for technical assistance. The studies reported herein were supported by the Irvin Krakoff Professor of Medicine Endowment (awarded to CFV), SPARK-VT program (awarded to JER and CFV), Lake Champlain Cancer Research Organization Research Fellowship (awarded to EAH), Nazarbayev University ORAU grant for Medicinal Electrochemistry (awarded to KL) and the Ministry of Education and Science of Kazakhstan (awarded to KL).

CONFLICTS OF INTEREST

The authors declare no potential conflicts of interest.

ORCID

Jon E. Ramsey http://orcid.org/0000-0001-6349-902X

REFERENCES

1. Yang S, et al. Pancreatic Q5 cancers require autophagy for tumor growth. *Genes Dev*. 2011;25:717–729.
2. Fan QW, et al. Akt and autophagy cooperate to promote survival of drug-resistant glioma. *Sci Signal*. 2010;3:ra81.
3. Degenhardt K, et al. Autophagy promotes tumor cell survival and restricts necrosis, inflammation, and tumorigenesis. *Cancer Cell*. 2006;10:51–64.
4. Ma XH, et al. Measurements of tumor cell autophagy predict invasiveness, resistance to chemotherapy, and survival in melanoma. *Clin Cancer Res*. 2011;17:3478–3489.

5. Xie X, White EP, Mehnert JM. Coordinate autophagy and mTOR pathway inhibition enhances cell death in melanoma. *PLoS ONE*. 2013;8:e55096.
6. Carew JS, et al. Targeting autophagy augments the anticancer activity of the histone deacetylase inhibitor SAHA to overcome Bcr-Abl-mediated drug resistance. *Blood*. 2007;110:313–322.
7. Ma XH, et al. Targeting ER stress-induced autophagy overcomes BRAF inhibitor resistance in melanoma. *J Clin Invest*. 2014;124:1406–1417.
8. Amaravadi RK, Thompson CB. The roles of therapy-induced autophagy and necrosis in cancer treatment. *Clin Cancer Res*. 2007;13:7271–7279.
9. Hollemans M, et al. Accumulation of weak bases in relation to intralysosomal pH in cultured human skin fibroblasts. *Biochim Biophys Acta*. 1981;643:140–151.
10. Gabourel JD. Effects of hydroxychloroquine on the growth of mammalian cells in vitro. *J Pharmacol Exp Ther*. 1963;141: 122–130.
11. Seitz C, et al. The dual PI3K/mTOR inhibitor NVP-BEZ235 and chloroquine synergize to trigger apoptosis via mitochondrial-lysosomal cross-talk. *Int J Cancer*. 2013;132:2682–2693.
12. Pellegrini P, et al. Acidic Q6extracellular pH neutralizes the autophagy-inhibiting activity of chloroquine: Implications for cancer therapies. *Autophagy*. 2014;10.
13. McAfee Q, et al. Autophagy inhibitor Lys05 has single-agent antitumor activity and reproduces the phenotype of a genetic autophagy deficiency. *Proc Natl Acad Sci U.S.A*. 2012;109: 8253–8258.
14. Solomon VR, Hu C, Lee H. Design and synthesis of chloroquine analogs with anti-breast cancer property. *Eur J Med Chem*. 2010; 45:3916–3923.
15. Hartinger CG, Dyson PJ. Bioorganometallic chemistry-from teaching paradigms to medicinal applications. *Chem Soc Rev*. 2009;38:391–401.
16. Dubar F, et al. The antimalarial ferroquine: role of the metal and intramolecular hydrogen bond in activity and resistance. *ACS Chem Biol*. 2011;6:275–287.
17. Top, S. et al. Synthesis, biochemical properties and molecular modelling studies of organometallic specific estrogen receptor modulators (SERMs), the ferrocifens and hydroxyferrocifens: evidence for an antiproliferative effect of hydroxyferrocifens on both hormone-Dependent and hormone-Independent Breast cancer cell lines. *Chem− A Euro J*. 2003;9:5223–5236.
18. Hartinger CG, Metzler-Nolte N, Dyson PJ. Challenges and opportunities in the development of organometallic anticancer drugs. *Organometallics*. 2012;31:5677–5685.
19. Lam K, Geiger WE. Synthesis and anodic electrochemistry of cymanquine and related complexes. *J Organomet Chem*. 2016;817: 15–20.
20. Geiger WE, et al., Patent-Cymanquine Q7compounds and derivatives thereof and use thereof, Worldwide, Editor. 2016.
21. Biot C, et al. Synthesis and antimalarial activity in vitro and in vivo of a new ferrocene-chloroquine analogue. *J Med Chem*. 1997;40: 3715–3718.
22. Verschraegen CF, et al. Specific organ metastases of human melanoma cells injected into the arterial circulation of nude mice. *Anticancer Res*. 1991;11:529–535.
23. Ishiguro K, Ando T, Goto H. Novel application of 4-nitro-7-(1-piperazinyl)-2, 1, 3-benzoxadiazole to visualize lysosomes in live cells. *Biotechniques*. 2008;45:465, 467–468.
24. Sheen JH, et al. Defective regulation of autophagy upon leucine deprivation reveals a targetable liability of human melanoma cells in vitro and in vivo. *Cancer Cell*. 2011;19:613–628.
25. Qiao S, et al. A REDD1/TXNIP pro-oxidant complex regulates ATG4B activity to control stress-induced autophagy and sustain exercise capacity. *Nat Commun*. 2015;6:7014.
26. Jackson WT, et al. Subversion of cellular autophagosomal machinery by RNA viruses. *PLoS Biol*. 2005;3:e156.
27. Wu K, et al. Anodic properties of diarylethene derivatives having organometallic piano-stool tags. *Chem Commun (Camb)*. 2011; 47:10109–10111.
28. King MA, Ganley IG, Flemington V. Inhibition of cholesterol metabolism underlies synergy between mTOR pathway inhibition and chloroquine in bladder cancer cells. *Oncogene*. 2016;35: 4518–4528.
29. Eng CH, et al. Macroautophagy is dispensable for growth of KRAS mutant tumors and chloroquine efficacy. *Proc Natl Acad Sci U.S.A*. 2016;113:182–187.
30. Kabeya Y, et al. LC3, GABARAP and GATE16 localize to autophagosomal membrane depending on form-II formation. *J Cell Sci*. 2004;117:2805–2812.
31. Mizushima N, Yoshimori T, Levine B. Methods in mammalian autophagy research. *Cell* 2010;140:313–326.
32. Mizushima N. Methods for monitoring autophagy. *Int J Biochem Cell Biol*. 2004;36:2491–2502.
33. Smalley KS, et al. Multiple signaling pathways must be targeted to overcome drug resistance in cell lines derived from melanoma metastases. *Mol Cancer Ther*. 2006;5: 1136– 1144.
34. Hather G, et al. Growth rate analysis and efficient experimental design for tumor xenograft studies. *Cancer Inform*. 2014;13:65–72.
35. Barnard RA, et al. Phase I clinical trial and pharmacodynamic evaluation of combination hydroxychloroquine and doxorubicin treatment in pet dogs treated for spontaneously occurring lymphoma. *Autophagy*. 2014;10:1415–1425.
36. Rangwala R, et al. Combined MTOR and autophagy inhibition: phase I trial of hydroxychloroquine and temsirolimus in patients with advanced solid tumors and melanoma. *Autophagy*. 2014;10:1391–1402.
37. Rangwala R, et al. Phase I trial of hydroxychloroquine with dose-intense temozolomide in patients with advanced solid tumors and melanoma. *Autophagy*. 2014;10:1369–1379.
38. Rosenfeld MR, et al. A phase I/II trial of hydroxychloroquine in conjunction with radiation therapy and concurrent and adjuvant temozolomide in patients with newly diagnosed glioblastoma multiforme. *Autophagy*. 2014;10:1359–1368.
39. Vogl DT, et al. Combined autophagy and proteasome inhibition: a phase 1 trial of hydroxychloroquine and bortezomib in patients with relapsed/refractory myeloma. *Autophagy*. 2014;10:1380–1390.
40. Held J, et al. Ferroquine and artesunate in African adults and children with Plasmodium falciparum malaria: a phase 2, multi-centre, randomised, double-blind, dose-ranging, non-inferiority study. *Lancet Infect Dis*. 2015;15:1409–1419.
41. McCarthy JS, et al. A Phase II pilot trial to evaluate safety and efficacy of ferroquine against early Plasmodium falciparum in an induced blood-stage malaria infection study. *Malar J*. 2016;15: 469.
42. Biot C, et al. Insights into the mechanism of action of ferroquine. Relationship between physicochemical properties and antiplasmodial activity. *Mol Pharm*. 2005;2: 185– 193.

43. Foley M, Tilley L. Quinoline antimalarials: mechanisms of action and resistance and prospects for new agents. *Pharmacol Ther*. 1998;79:55–87.
44. Fox RI. Mechanism of action of hydroxychloroquine as an antirheumatic drug. *Semin Arthritis Rheum*. 1993;23:82–91.
45. Lamphier M, et al. Novel small molecule inhibitors of TLR7 and TLR9: mechanism of action and efficacy in vivo. *Mol Pharmacol*. 2014;85:429–440.
46. Schmitz KJ, et al. Pognostic relevance of autophagy-related markers LC3, p62/sequestosome 1, Beclin-1 and ULK1 in colorectal cancer patients with respect to KRAS mutational status. *World J Surg Oncol*. 2016;14:189.
47. Giatromanolaki A, et al. Autophagy and lysosomal related protein expression patterns in human glioblastoma. *Cancer Biol Ther*. 2014;15:1468–1478.
48. Giatromanolaki A, et al. Autophagy proteins in prostate cancer: relation with anaerobic metabolism and Gleason score. *Urol Oncol*. 2014;32: 39 e11–e18.
49. Choi J, Jung W, Koo JS. Expression of autophagy-related markers beclin-1, light chain 3A, light chain 3B and p62 according to the molecular subtype of breast cancer. *Histopathology*. 2013;62:275–286.
50. Goulielmaki M, et al. BRAF associated autophagy exploitation: bRAF and autophagy inhibitors synergise to efficiently overcome resistance of BRAF mutant colorectal cancer cells. *Oncotarget* 2016;7:9188–9221.

Graphical Abstract

The contents of this page will be used as part of the graphical abstract of html only. It will not be published as part of main.

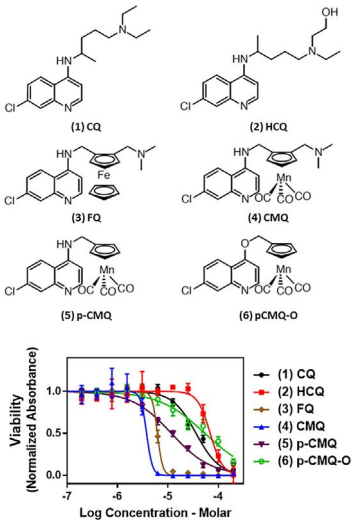

The cellular process of autophagy has emerged as a viable target in the treatment of many tumor types. Efforts are underway to optimize the anti-malarial compound, chloroquine, to improve its ability to block autophagy in the fight against cancer. Here, we report a novel organometallic derivative of chloroquine, termed Cymanquine, that displays improved anti-autophagy properties, and the capacity to slow tumor growth in vivo.